

# On the globular cluster formation history of NGC 5128

S. Kaviraj\*, I. Ferreras<sup>1,2</sup>, S.-J. Yoon<sup>1</sup> and S. K. Yi<sup>1</sup>

<sup>1</sup>Department of Physics, University of Oxford, Keble Road, Oxford OX1 3RH

<sup>2</sup>Department of Physics, Institute of Astronomy, ETH Hoenggerberg HPF D8, 8093 Zurich, Switzerland

16 December 2003

## ABSTRACT

We deduce the globular cluster formation history of the nearby elliptical NGC 5128 by using a phenomenological chemical enrichment model to reproduce its observed metallicity distribution function (MDF). We derive the observed MDF using recently obtained *U* and *B* photometry of the NGC 5128 GC system, with  $(U - B)$  used as the metallicity indicator. We test whether the observed MDF can be reproduced using a single starburst at high redshift followed by passive evolution (monolithic scenario). Our results strongly indicate that this scenario is incapable of reproducing the observed MDF of the NGC 5128 GC system. At least one more major starburst is required. A persistent feature of our best-fit models is a strong GC formation episode in the first 1-2 Gyrs, followed by a second formation episode typically after 10-12 Gyrs. Roughly one-third of the stellar mass in the GC system is created in this late starburst, producing clusters that are potentially less than 1 Gyr old. Although we do not have adequate resolution in the model or in the observed MDF to make a reliable claim about the possibility of additional GC formation episodes, our results suggest that the GCs in this galaxy did not form solely in a monolithic collapse and seem to support observational evidence which indicates that NGC 5128 is a merger remnant.

**Key words:** galaxies: elliptical and lenticular, cD – galaxies: evolution – galaxies: formation – galaxies: individual: NGC 5128

## 1 INTRODUCTION

Globular cluster (GC) systems have been popular tools in deciphering the star formation histories (SFHs) of galaxies. Their ubiquitous presence in galaxies of all morphological types, coupled with evidence that their creation seems to accompany major star formation episodes (e.g. Larsen & Richtler 1999; Ho 1997) makes them useful tracers of galactic evolution (e.g. Kissler-Patig et al. 1998; van den Bergh 2000; Yoon & Lee 2002). In addition, GC systems are well represented by simple stellar populations (SSPs) with stars of the same age and chemical composition, which makes them easy to study using SSP models (e.g. Yi et al. 2004).

The exact formation mechanism of GCs has been the subject of much recent debate. Many models for GC formation have been proposed including gaseous mergers (Ashman & Zepf 1992), in situ formation (e.g. Harris et al. 1995), multiphase collapse (Forbes et al. 1997), tidal stripping (e.g. Cote et al. 1998) and hierarchical clustering (Beasley et al. 2003). While none of these models can be conclusively excluded, the widespread discovery of multimodal metallicity distributions in GC populations effectively rules out an extreme version of the monolithic collapse scenario for their

formation (Forbes et al. 1997). Furthermore, the correlation between the mean metallicity of GCs and galaxy luminosity (e.g. Forbes et al. 1996; Durrell et al. 1996) indicates that chemical enrichment of the GC system is intimately linked to the evolution of the host galaxy (Forbes & Forte 2001), a point that largely motivates this case-study.

The object of this study is NGC 5128, the giant elliptical galaxy in the nearby Centaurus Group (see Israel 1998, for a comprehensive review of NGC 5128). Located at a distance of approximately 3.6 Mpc (e.g. Soria et al. 1996), NGC 5128 is the closest giant elliptical system with an estimated GC population of  $1550 \pm 350$  (Harris et al. 1984). It has been widely studied not only because of its proximity and relative brightness, but also because it displays unusual physical features which suggest that this galaxy is a post-merger remnant. A prominent dust lane which contains young stars and HII regions (e.g. Unger et al. 2000; Wild & Eckart 2000) and a series of optical shells (Malin & Carter 1983) which have HI (Schiminovich et al. 1994) and molecular CO (Charmandaris et al. 2000) gas associated with them, are considered strong evidence that NGC 5128 underwent a recent merger event within the last  $10^9$  years. Recently, Rejkuba et al. (2004) suggest that star formation may have stopped as recently as 2 Myr ago in the north-eastern shell of NGC 5128 and that the last merger

\* E-mail: skaviraj@astro.ox.ac.uk

event for this galaxy may have been only 100 Myr ago. If the monolithic collapse picture of elliptical galaxy formation (e.g. Eggen et al. 1962; Tinsley 1972; Larson 1974; Chiosi & Carraro 2002) turns out to be inaccurate then it is possible that such characteristics are the norm rather than the exception for elliptical systems. NGC 5128 therefore provides an ideal laboratory in which to investigate such phenomena and test the monolithic formation scenario for elliptical galaxies.

In this study we deduce the formation history of the GC system of NGC 5128, by attempting to reproduce its observed metallicity distribution function (MDF) using a phenomenological chemical enrichment model (see Beasley et al. 2003, for similar work using a semi-analytical model). We derive the observed MDF of this elliptical galaxy using recently obtained  $U$  and  $B$  photometry of 207 clusters in its GC system (Peng et al. 2003). ( $U - B$ ) is used as the metallicity indicator (Yi et al. 2004). We note that our choice of using metallicities rather than ages is due to the fact that age determinations using age-sensitive colours, e.g. ( $B - V$ ), are subject to substantially larger uncertainties than similar derivations of metallicity using ( $U - B$ ). Moreover, the use of a consistent chemical enrichment code means that we can effectively transform metallicities into ages.

We are interested in exploring whether a single starburst followed by passive evolution (a monolithic scenario) is capable of reproducing the formation history of the NGC 5128 GCs. We compare the results for this single starburst analysis to a double starburst scenario, analysing positions, temporal spreads and relative strengths of the two star formation episodes that best explain the MDF of the NGC 5128 GC system. Having obtained best-fit models to the observed MDF, we use our stellar models to derive a synthetic spectral energy distribution (SED) and compare broad-band colours computed from this model SED to NGC 5128 photometric data. This allows us to explore the correlation, if any, between the bulk star formation history in this galaxy and the formation history of the GC system suggested by our chemical enrichment model.

## 2 DERIVATION OF THE OBSERVED NGC 5128 MDF

We derive the observed MDF for the NGC 5128 GC system by using photometric data in the  $U$  and  $B$  bands. We compute the metallicities by overlaying a model ( $U - B$ ) vs. ( $B - V$ ) grid on the GC data, with ( $U - B$ ) used as the metallicity indicator. The behaviour of ( $U - B$ ) and its potential as a robust indicator of metallicity, in the context of the data used in this paper, is explored in detail in Yi et al. (2004).

The metallicity of each GC is computed by identifying its two bounding iso-metallicity curves followed by linear interpolation between them. We do not use the same iso-metallicity curves to compute the metallicity error from the ( $U - B$ ) errors. Instead we treat each error limit as a separate *point* on the grid and repeat the process described above. Given the irregular spacing and pseudo-horizontal nature of the model iso-metallicity curves (see Figure 7 in Yi et al. 2004), this results in a more accurate approximation

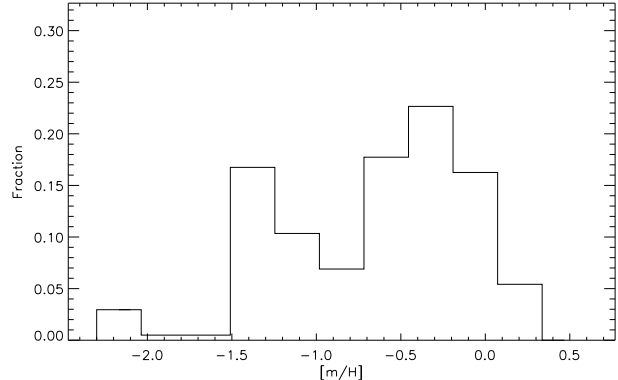


**Figure 1.** Metallicity distribution derived from ( $U - B$ ) colours of 69 GCs which have ( $U - B$ ) photometric errors less than 0.1 mag.

of the metallicity errors for each GC.

## 3 GC SELECTION

Our photometric data on NGC 5128 contains 207 GCs, some of which suffer from extremely large uncertainties in the reported  $U$  and  $B$  magnitudes. In this study we have applied a cut of 0.1 mag to the uncertainty in ( $U - B$ ), retaining 69 GCs out of the original sample of 207. The reasons for applying a rather stringent magnitude cut are two fold. Firstly, some GCs have extremely large photometric errors. By using GCs with small error bars we are able to better quantify the metallicity of the GCs that we eventually use and their associated errors.

Secondly, having performed this magnitude cut we find, rather fortuitously, that the MDF for the entire sample of 207 GCs is very similar to our reduced sample; a Kolmogorov-Smirnov (KS) test between the entire sample and the distribution derived after the uncertainty cut indicates that the two samples are consistent at the 95 percent confidence level.

Our aim is to maximise the *accuracy* of our analysis and the magnitude cut we employ increases the robustness of our final solutions, without transforming the original distribution significantly. Figure 1 presents the metallicity distribution derived from the ( $U - B$ ) colours of our final sample of clusters. We note that our derived MDF is consistent with the NGC 5128 MDF derived using the ( $C - T_1$ ) index for 205 clusters in Harris et al. (2003).

## 4 STAR FORMATION AND GAS INFALL PRESCRIPTIONS

Feedback processes from star formation remain poorly understood. Supernovae typically inject large amounts of energy into the inter-stellar medium (ISM). The energy deposited can be either kinetic or thermal and the exact description of these processes remains the subject of much de-

bate (see e.g. Katz 1992; Mihos & Hernquist 1994; Yepes et al. 1997; Ferreras et al. 2002; Silk 2003). Such feedback processes can interrupt or accelerate star formation, so that the simple coupling between star formation and the gas density implied by a Schmidt law (Schmidt 1959) may be incorrect. In this model, we decouple the star formation rate from the gas density in the system to qualitatively account for such feedback processes from star formation. We take the star formation rate to be a sequence of gaussian functions independent of the gas density

$$\Psi(t) = \sum_n \frac{f_n}{\sqrt{2\pi}\sigma_n} \exp \frac{-(t - \tau_n)^2}{2\sigma_n^2} \quad (1)$$

In Equation 1  $f_n$  is the normalisation amplitude,  $\sigma_n$  is the temporal spread and  $\tau_n$  is the centre-point of starburst  $n$ . With the gaussian starbursts normalised as shown above, we keep the total area under  $\Psi(t)$  and hence the total stellar mass equal to 1 by ensuring that  $\sum_n f_n = 1$ . We have checked that our results do not depend strongly on our choice of mathematical function by repeating our analysis using lorentzian starbursts. We find that our conclusions remain unchanged.

We assume that the system begins with no gas and use an exponentially decaying gas infall rate

$$g_{in}(t) = \frac{\eta}{\tau_{in}} \exp \left( \frac{-t}{\tau_{in}} \right) \quad (2)$$

Here  $\tau_{in}$  is the infall timescale and  $\eta$  is a parameter that controls the final gas fraction in the system and is defined below. Noting that,

$$\int_0^{t_U} g_{in}(t) dt = \eta \left[ 1 - \exp \left( \frac{-t_U}{\tau_{in}} \right) \right] \approx \eta \quad (3)$$

where  $t_U$  is the age of the universe in Gyrs, we can force the system to have a final gas fraction  $g_{frac}$  by choosing

$$g_{frac} = \frac{\eta - 1}{\eta} \quad (4)$$

so that

$$\eta = \frac{1}{1 - g_{frac}} \quad (5)$$

We fix the infall timescale  $\tau_{in}$  to 5 Gyrs which leaves the following  $3n$  free parameters in the model for an  $n$  starburst scenario

$$(f_1, \dots, f_{n-2}, \tau_1, \dots, \tau_{n-1}, \sigma_1, \dots, \sigma_{n-1}, g_{frac})$$

We note that due to the decoupling of the star formation rate from gas density, changing the value of the  $\tau_{in}$  has no impact on our subsequent analysis. Essentially, the behaviour of the system remains unchanged as long as there is a reservoir of gas available to make stars.

## 5 DERIVATION OF BEST FIT PARAMETERS

We begin our analysis by studying a single starburst scenario which describes a monolithically evolving system. We then refine our analysis by adding another starburst and then check that small perturbations to the major star formation episodes do not affect the best-fit values for our

parameters. This sequence is repeated for four final gas fractions -  $g_{frac} = 0.1, 0.2, 0.35, 0.5$ . Since we are modelling an elliptical galaxy, the value of  $g_{frac}$  is likely to be low, probably somewhere in the region  $0.1 - 0.35$ . In a recent work, Sanderson et al. (2003) find the (hot) gas fraction in ellipticals within  $R_{200}$  to be approximately 0.1.

We compare the distributions of stellar mass predicted by our model with the observed GC distribution using the Kolmogorov-Smirnov (KS) test. The *best-fit* values of these quantities are calculated by marginalising their KS probabilities, which involves summing (integrating) out the probability dependence of all other parameters, leaving a probability distribution for each parameter which is independent of all others in the model. For example, in a double starburst scenario, the marginalised probability distribution for the parameter  $\tau_1$  is calculated as

$$P(\tau_1) = \varsigma \sum_{i,j,k} P(\tau_1, \tau_{2i}, \sigma_{1j}, \sigma_{2k}) \quad (6)$$

where  $\varsigma$  is a normalising constant which ensures that  $P(\tau_1)$  integrates to 1. This probability distribution will not, in general, be symmetric and therefore should not be approximated by a gaussian.

We take the best fit value of a parameter as the value at which its marginalised probability function peaks. In addition, we *define* errors for these parameters that are superficially similar to the *one-sigma* errors frequently used for gaussian probability distributions. If  $X$  is the most likely value of a parameter  $x$ , then we define the positive error,  $x_+$ , as

$$\int_X^{x_+} P(x) dx = 0.34 \int_X^{\infty} P(x) dx \quad (7)$$

and similarly the negative error,  $x_-$ , as

$$\int_{x_-}^X P(x) dx = 0.34 \int_{-\infty}^X P(x) dx \quad (8)$$

Finally, given the fact that each GC has a metallicity error associated with it, we check that the positions of the most likely values for our model parameters are robust with respect to these errors. We perform this check by adding random noise to our observed MDF and producing KS values for these *noisy* MDFs. The noise is added by running through each GC and changing its metallicity to one of its error points *randomly*. This process is repeated a hundred times to generate a hundred noisy MDFs. We have checked that the KS values do not deviate significantly from the fiducial value and find that the KS values are suitably robust (within 8 percent of the original values) when the fiducial MDF is perturbed in this way. This is mainly a result of choosing GCs with small photometric errors.

## 6 RESULTS AND ANALYSIS

### 6.1 Single and double starburst models

For a single starburst scenario, the maximum KS probability we achieve in our model is around 2 percent, significantly lower than the double starburst scenarios we explore later. Apart from the absolute KS value, we shall be interested in

the *relative KS values* between different models, as a measure of the *comparative goodness of fit* between scenarios. The single starburst model fails to reproduce, with any acceptable accuracy, the observed metallicity distribution of NGC 5128 and we conclude that the evolution of NGC 5128 is very unlikely to have been monolithic.

We now refine our analysis by adding a second starburst, which produces a six dimensional parameter space with the star formation rate as the sum of two gaussians

$$\Psi(t) = \frac{f_1}{\sqrt{2\pi}\sigma_1} \exp \frac{-(t-\tau_1)^2}{2\sigma_1^2} + \frac{1-f_1}{\sqrt{2\pi}\sigma_2} \exp \frac{-(t-\tau_2)^2}{2\sigma_2^2} \quad (9)$$

We note that for the same range of values for  $(\tau_1, \tau_2, \sigma_1, \sigma_2)$  this star formation rate is symmetric with respect to the exchange of indices  $1 \leftrightarrow 2$ , so that we need to explore the  $f_1$  parameter space only in the region  $0 - 0.5$ . Table 1 shows the best-fit values for the starburst parameters  $(f_1, f_2, \tau_1, \tau_2, \sigma_1, \sigma_2)$  for final gas fractions of 0.5 to 0.1.

The crucial discriminant between the monolithic and double starburst pictures is the *relative KS probability* generated by these models. In Figure 2, we present the best KS values produced in the double starburst models. The single starburst case is shown, for comparison, by the solid line at 2 percent. In Figure 3 we present three star formation histories (SFHs) which yield the highest KS probabilities (see shaded region in Figure 2) by showing SFHs for favoured values  $(f_1, f_2)$  in a system with a final gas fraction of 0.35.

It is clear that a double starburst model is *significantly* preferred to a monolithic scenario. Figure 2 suggests that an intermediate gas fraction of 0.35 with  $(f_1, f_2) = (0.35, 0.65)$  is the most favoured model, so that roughly one-third of the stellar mass is predicted to have formed in a late starburst centred at around 11 Gyrs. The shaded region in Figure 2 shows a set of degenerate solutions for models producing high KS values, all of which reasonably reproduce the observed NGC 5128 MDF and therefore cannot be completely discounted. All points within this region have  $f_1 = 0.35 - 0.5$ . Changing the relative sizes of the starburst even further results in the KS probability declining rapidly. This is clearly expected, since in the limit  $f_1 \rightarrow 0$ , we recover a single starburst, which we have already established as being incapable of reproducing the observed NGC 5128 MDF.

## 6.2 Perturbations to the double starburst case

As mentioned above, the  $n$  starburst scenario contains  $3n$  free parameters. Clearly, as we make more free parameters available to the model, we should expect to do better in terms of matching the observed NGC 5128 MDF. We note first that the KS values from the double starburst scenarios are significantly large. Refining the model further would not make an appreciable difference to the KS probabilities, certainly not as much as in the transition from the single to the double starburst case. In addition, given the errors in the observed MDF and the resolution of our model, further refinement would not provide much greater insight into the star formation history of this galaxy.

Therefore, instead of repeating the study above with a wholesale three starburst analysis, we choose to treat the third starburst as a perturbation on the double starburst

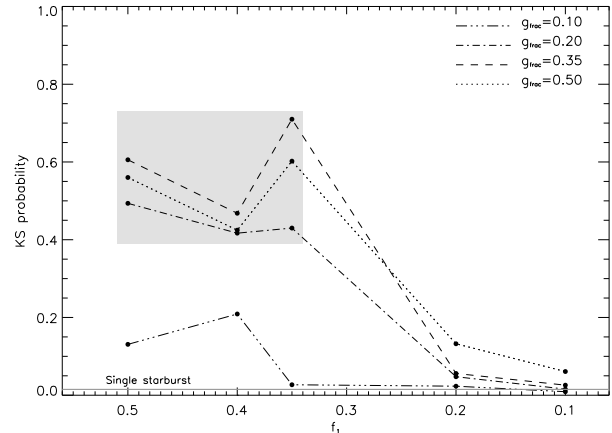


**Figure 2.** Best KS probabilities for various values of  $f_1$  and for four final gas fractions  $g_{frac}$ . The shaded region shows a set of degenerate models which have high KS probabilities and therefore cannot be discounted completely. The KS probability for a single starburst scenario is shown by the solid line at 2 percent

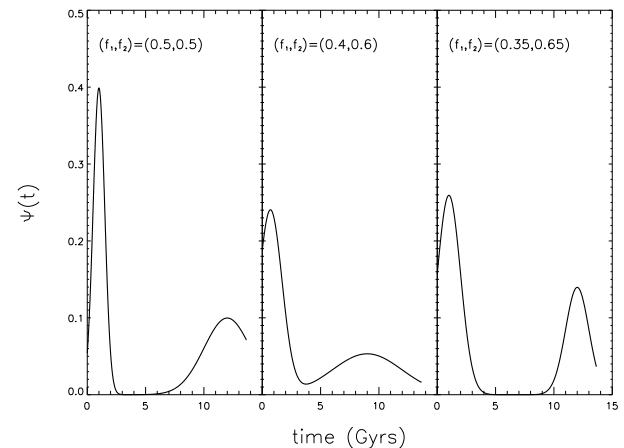


**Figure 3.** Three star formation histories corresponding to the best KS probabilities shown in the shaded region in Figure 2.

system. We are interested in studying how the KS probabilities change if we apply a small perturbation to each of the major star forming episodes. This simple perturbation analysis will give an indication of how localised these double starburst KS hotspots are in the nine parameter triple starburst space.

Figure 4 shows the best KS values achieved after applying a 5 percent perturbation i.e.  $f_{perturb} = 0.05$  as a *fraction* of the best KS values in the corresponding unperturbed double starburst scenario. In almost all cases the KS value improves slightly, but crucially it does not deviate much from the double starburst case. We conclude from this analysis that the KS hotspot is *not* extremely localised in the nine parameter triple starburst space and appears to be stable at least under perturbations of sizes 5 percent and below. Although we have sampled only a small fraction of this nine-dimensional parameter space, the resistance to small

**Table 1.** Best-fit values and errors for the double starburst scenarios with final gas fractions in the range 0.1 – 0.5.

		Final gas fraction = 0.5			
$(f_1, f_2)$	(0.5, 0.5)	(0.4, 0.6)	(0.35, 0.65)	(0.2, 0.8)	(0.1, 0.9)
$\tau_1$	$0.72_{-0.31}^{+0.12}$	$9.99_{-0.26}^{+0.46}$	$10.00_{-1.00}^{+0.44}$	$11.90_{-0.96}^{+0.13}$	$11.10_{-0.95}^{+0.25}$
$\tau_2$	$5.00_{-0.26}^{+0.22}$	$1.00_{-0.14}^{+0.09}$	$0.51_{-0.02}^{+0.18}$	$1.01_{-0.04}^{+0.13}$	$1.00_{-0.21}^{+0.14}$
$\sigma_1$	$0.70_{-0.12}^{+0.01}$	$3.58_{-0.17}^{+0.24}$	$1.99_{-0.25}^{+0.80}$	$0.60_{-0.02}^{+1.02}$	$1.49_{-0.23}^{+0.17}$
$\sigma_2$	$3.55_{-0.27}^{+0.21}$	$0.70_{-0.03}^{+0.15}$	$1.00_{-0.05}^{+0.12}$	$1.02_{-0.08}^{+0.23}$	$2.00_{-0.09}^{+0.13}$

		Final gas fraction = 0.35			
$(f_1, f_2)$	(0.5, 0.5)	(0.4, 0.6)	(0.35, 0.65)	(0.2, 0.8)	(0.1, 0.9)
$\tau_1$	$11.40_{-0.54}^{+0.07}$	$9.00_{-0.93}^{+0.07}$	$12.00_{-0.93}^{+0.07}$	$9.00_{-0.88}^{+0.83}$	$12.10_{-0.92}^{+0.62}$
$\tau_2$	$1.00_{-0.09}^{+0.20}$	$1.00_{-0.09}^{+0.20}$	$1.00_{-0.06}^{+0.20}$	$1.00_{-0.06}^{+0.23}$	$1.00_{-0.09}^{+0.20}$
$\sigma_1$	$0.70_{-0.04}^{+0.16}$	$3.00_{-0.28}^{+0.36}$	$0.99_{-0.15}^{+0.48}$	$3.08_{-0.55}^{+0.36}$	$3.05_{-0.73}^{+0.36}$
$\sigma_2$	$3.02_{-0.93}^{+0.38}$	$1.10_{-0.09}^{+0.20}$	$1.13_{-0.09}^{+0.19}$	$1.99_{-0.22}^{+0.31}$	$2.99_{-0.42}^{+0.28}$

		Final gas fraction = 0.2			
$(f_1, f_2)$	(0.5, 0.5)	(0.4, 0.6)	(0.35, 0.65)	(0.2, 0.8)	(0.1, 0.9)
$\tau_1$	$0.99_{-0.04}^{+0.15}$	$11.45_{-0.48}^{+0.19}$	$11.20_{-0.61}^{+0.15}$	$10.90_{-1.32}^{+0.24}$	$10.70_{-1.46}^{+0.24}$
$\tau_2$	$10.50_{-0.88}^{+0.33}$	$1.00_{-0.06}^{+0.11}$	$1.01_{-0.04}^{+0.13}$	$0.99_{-0.04}^{+0.15}$	$1.00_{-0.04}^{+0.16}$
$\sigma_1$	$0.76_{-0.05}^{+0.19}$	$1.74_{-0.27}^{+0.31}$	$1.00_{-0.10}^{+0.37}$	$2.00_{-0.22}^{+0.38}$	$2.50_{-0.20}^{+0.66}$
$\sigma_2$	$3.50_{-0.18}^{+0.23}$	$0.99_{-0.06}^{+0.11}$	$1.00_{-0.07}^{+0.14}$	$2.00_{-0.15}^{+0.19}$	$2.99_{-0.61}^{+0.14}$

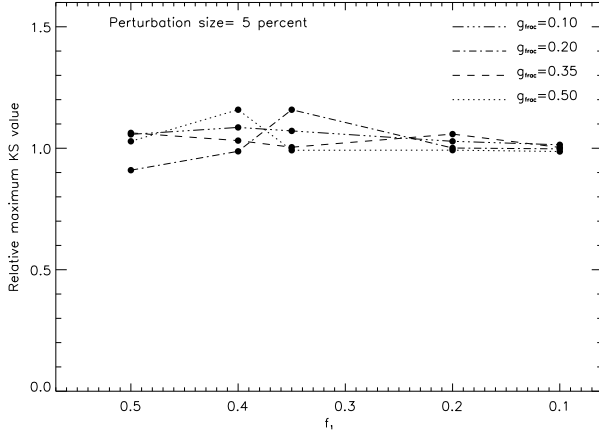
  

		Final gas fraction = 0.1			
$(f_1, f_2)$	(0.5, 0.5)	(0.4, 0.6)	(0.35, 0.65)	(0.2, 0.8)	(0.1, 0.9)
$\tau_1$	$1.12_{-0.12}^{+0.11}$	$12.06_{-0.28}^{+0.15}$	$11.40_{-0.87}^{+0.11}$	$12.00_{-0.78}^{+0.56}$	$10.89_{-0.80}^{+0.14}$
$\tau_2$	$11.20_{-0.78}^{+0.15}$	$0.91_{-0.67}^{+0.12}$	$1.45_{-0.12}^{+0.20}$	$1.20_{-0.12}^{+0.18}$	$1.00_{-0.34}^{+0.18}$
$\sigma_1$	$0.72_{-0.18}^{+0.29}$	$3.46_{-0.17}^{+0.23}$	$2.00_{-0.30}^{+0.17}$	$1.00_{-0.12}^{+0.36}$	$3.00_{-0.18}^{+0.56}$
$\sigma_2$	$3.53_{-0.58}^{+0.28}$	$0.99_{-0.03}^{+0.12}$	$1.00_{-0.05}^{+0.11}$	$3.00_{-0.06}^{+0.29}$	$2.50_{-0.35}^{+0.10}$

perturbations indicates that the double burst scenarios are reasonably stable and robust solutions.

## 7 FORMATION HISTORIES: GC SYSTEM VS. BULK OF STELLAR MASS

We now study whether the formation history of the GC system suggested by the best-fit model is similar to the bulk star formation history of the galaxy. Figure 5 shows the fraction of the total stellar mass in the GC system over a range



**Figure 4.** KS values for perturbed double starburst scenarios as a fraction of the KS values in the unperturbed case. The size of the perturbation applied to the system is 5 percent.

	GC model	Observed
$(U - B)$	0.31	0.41 <sup>a</sup>
$(B - V)$	0.75	0.88 <sup>b</sup>
$(V - K)$	2.58	2.79 <sup>d</sup>

**Table 2.** Derived colours from best-fit GC model SED compared with observed photometry of NGC 5128. <sup>a</sup> Integrated  $(U - B)$  colour from main body of galaxy (van den Bergh 1976) <sup>b</sup> Integrated  $(B - V)$  colour (de Vaucouleurs et al. 1991), <sup>c</sup> integrated  $(V - K)$  colour (Pahre 1999).

of ages and metallicities. We convolve our SSP models (Yi et al. 1997) with this *age-metallicity grid* to generate a synthetic spectral energy distribution (SED), by summing up the SEDs for each cell in the grid and weighting them by the fraction of stellar mass that appears in that cell. By comparing colours derived from this synthetic SED with photometric data for NGC 5128, we could infer the existence of any correlation between the GC formation history and the bulk star formation history of NGC 5128. This comparison is shown in Table 2.

It is worth noting that NGC 5128 is known to lie blue-ward of colours observed in normal giant elliptical galaxies. The difference in the  $(U - B)$  and  $(B - V)$  colours between the main body of NGC 5128 and normal giant ellipticals are typically  $\delta(U - B) \sim 0.15$  and  $\delta(B - V) \sim 0.08$  (van den Bergh 1976; Israel 1998). We see from Table 2 that the predicted model colours are consistently bluer than that suggested in the optical photometry. This indicates that the formation history of the GC system suggested by the model produces colours which are inconsistent with the stellar populations in the main body of the galaxy. This suggests that there is not a one-to-one correlation between the bulk star formation history of this galaxy and the formation history of its GC system. However, we should note that the full complement of GCs in this galaxy may produce a model SED which is slightly different, which in turn will affect the values in Table 2.

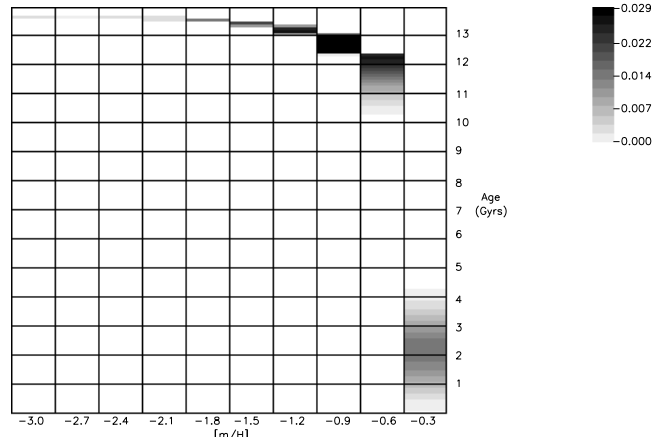


**Figure 5.** Age-metallicity grid showing the fraction of stellar mass predicted by the chemical enrichment model as a function of age and metallicity. The key indicates stellar fractions corresponding to the levels of shading in the plot.

## 8 DISCUSSION AND CONCLUSIONS

We have studied the observed MDF of the GC system in the elliptical galaxy NGC 5128 using a phenomenological chemical enrichment model. Our results show that the GCs in this galaxy are extremely unlikely to have evolved monolithically as a result of a single starburst followed by passive evolution. The models seem to indicate that at least another major star formation episode is required, although we do not have adequate resolution in the model or in the observed MDF to make any reliable claim about the possibility of additional GC formation episodes.

The double starburst analysis produces high KS probabilities and therefore good fits to the observed MDF, with a majority of best-fit models (shaded region in Figure 2) favouring an initial GC formation episode in the first 1-2 Gyrs, followed by a second late formation episode typically after 10-12 Gyrs. The late starburst results in a small fraction ( $\sim 5$  percent) of the stellar mass in the GC system having ages *less than 1 Gyr*. If NGC 5128 has over 1500 clusters, then we might expect a handful of those clusters to have ages less than 1 Gyr. Unfortunately, broad-band colours are not reliable age indicators, so any confirmation of such young clusters shall rely on the use of more robust age indicators such as Balmer line indices (e.g.  $H_\beta$ ). We note that the integrated GC SED predicted by the best-fit model yields colours that are consistently bluer than NGC 5128 photometry in the optical and infra-red wavelengths, suggesting that the GC formation history is not strongly correlated to the history of bulk star formation in this galaxy, although a definite conclusion is hampered by the incomplete nature of our GC dataset.

We have not made any *a priori* assumptions about the driving mechanisms behind star formation episodes in our model. While a single starburst followed by passive evolution can be discounted, the phenomenological nature of our model admits any other scenario where two star formation episodes are possible. Our results are in general agreement with Beasley et al. (2003) who obtain good fits to the observed NGC 5128 MDF using a semi-analytical galaxy

formation model with metal-poor GC formation halted at  $z \sim 5$ . These results taken together provide a strong theoretical argument against the monolithic formation of this galaxy, a result which is in agreement with the large body of observational evidence that has long indicated that it is a post-merger remnant.

## ACKNOWLEDGEMENTS

We thank Eric Peng for providing the NGC 5128 data on which this work is based. We are grateful to Roger Davies, Joseph Silk and Julien Devriendt for their careful reading of this manuscript and numerous constructive comments. SK acknowledges PPARC grant PPA/S/S/2002/03532. This research has been supported by PPARC Theoretical Cosmology Rolling Grant PPA/G/O/2001/00016 (S. K. Yi and I. Ferreras), the Glasstone Fellowship and the Post-doctoral Fellowship Program of Korea Science & Engineering Foundation (S.-J. Yoon) and has made use of Starlink computing facilities at the University of Oxford.

## REFERENCES

Ashman K. M., Zepf S. E., 1992, ApJ, 384, 50  
 Beasley M. A., Harris W. E., Harris G. L. H., Forbes D. A., 2003, MNRAS, 340, 341  
 Charmandaris V., Combes F., van der Hulst J. M., 2000, AAP, 356, L1  
 Chiosi C., Carraro G., 2002, MNRAS, 335, 335  
 Cote P., Marzke R. O., West M. J., 1998, ApJ, 501, 554  
 de Vaucouleurs G., de Vaucouleurs A., Corwin H. G., Buta R. J., Paturel G., Fouque P., 1991, Third Reference Catalogue of Bright Galaxies. Volume 1-3, XII, 2069 pp. 7 figs.. Springer-Verlag Berlin Heidelberg New York  
 Durrell P. R., Harris W. E., Geisler D., Pudritz R. E., 1996, AJ, 112, 972  
 Eggen O. J., Lynden-Bell D., Sandage A. R., 1962, ApJ, 136, 748  
 Ferreras I., Scappapietra E., Silk J., 2002, ApJ, 579, 247  
 Forbes D. A., Brodie J. P., Grillmair C. J., 1997, AJ, 113, 1652  
 Forbes D. A., Forte J. C., 2001, MNRAS, 322, 257  
 Forbes D. A., Franx M., Illingworth G. D., Carollo C. M., 1996, ApJ, 467, 126  
 Harris G. L. H., Geisler D., Harris W. E., Hesser J. E., Reid M., Milne M., Hulme S. C., Kidd T. T., Schmidt B. P., 2003, in Extragalactic Globular Cluster Systems, Proceedings of the ESO Workshop held in Garching, Germany, 27-30 August 2002, p. 113. Uncovering the NGC 5128 Globular Cluster System. pp 113  
 Harris G. L. H., Hesser J. E., Harris H. C., Curry P. J., 1984, ApJ, 287, 175  
 Harris W. E., Pritchett C. J., McClure R. D., 1995, ApJ, 441, 120  
 Ho L. C., 1997, in Revista Mexicana de Astronomia y Astrofisica Conference Series pp 5  
 Israel F. P., 1998, AAPR, 8, 237  
 Katz N., 1992, ApJ, 391, 502  
 Kissler-Patig M., Forbes D. A., Minniti D., 1998, MNRAS, 298, 1123  
 Larsen S. S., Richtler T., 1999, AAP, 345, 59  
 Larson R. B., 1974, MNRAS, 166, 385  
 Malin D. F., Carter D., 1983, ApJ, 274, 534  
 Mihos J. C., Hernquist L., 1994, ApJ, 437, 611  
 Pahre M. A., 1999, ApJS, 124, 127  
 Peng E. W., Ford H. C., Freeman K. C., White R. L., 2003, AJ, in press  
 Rejkuba M., Greggio L., Zoccali M., 2004, astro-ph/0401304  
 Sanderson A. J. R., Ponman T. J., Finoguenov A., Lloyd-Davies E. J., Markevitch M., 2003, MNRAS, 340, 989  
 Schiminovich D., van Gorkom J. H., van der Hulst J. M., Kasow S., 1994, ApJL, 423, L101  
 Schmidt M., 1959, ApJ, 129, 243  
 Silk J., 2003, MNRAS, 343, 249  
 Soria R., Mould J. R., Watson A. M., Gallagher J. S., Ballester G. E., Burrows C. J., Casertano S., Clarke J. T., Crisp D., Griffiths R. E., Hester J. J., Hoessel J. G., Holtzman J. A., Scowen P. A., Stapelfeldt K. R., Trauger J. T., Westphal J. A., 1996, ApJ, 465, 79  
 Tinsley B. M., 1972, ApJ, 178, 319  
 Unger S. J., Clegg P. E., Stacey G. J., Cox P., Fischer J., Greenhouse M., Lord S. D., Luhman M. L., Satyapal S., Smith H. A., Spinoglio L., Wolfire M., 2000, AAP, 355, 885  
 van den Bergh S., 1976, ApJ, 208, 673  
 van den Bergh S., 2000, PASP, 112, 932  
 Wild W., Eckart A., 2000, AAP, 359, 483  
 Yepes G., Kates R., Khokhlov A., Klypin A., 1997, MNRAS, 284, 235  
 Yi S., Demarque P., Oemler A. J., 1997, ApJ, 486, 201  
 Yi S. K., Peng E. W., Freeman K. C., Kaviraj S., Yoon S. -J., 2004, MNRAS, in press; astro-ph/0401454  
 Yoon S. -J., Lee Y. -W., 2002, Science, 297, 578